Power Quality Assessment of Renewable Energy Sources Integration on MV Networks.

Francis Itote, George Irungu, Michael Saulo

Abstract— The amount of energy harnessed from Renewable energy sources (RES) is constantly increasing. This rise can be attributed to technological advancement that has lowered generation costs, financing from governments and private sector, efficient payment plans (e.g. Pay As You Go), and need for clean energy. RES are either integrated into the local distribution grids or used as standalone/off grid solutions that facilitate easy energy access to meet the ever-increasing power requirements. Extensive studies on the behavior of power networks integrated with RES is therefore required so as to facilitate the changes that will be made on the current grid configuration. This study assessed the impact on the harmonics and flicker of distributed networks due to the integration of wind and solar energy sources. To achieve this, the IEEE-33 bus system was integrated with RES at selected locations and power quality and harmonic analysis performed using DigSILENT PowerFactory software. Results obtained indicate increased harmonic and flicker levels of distribution networks. The levels of harmonic distortion and flicker obtained were found to be reliant on the type, penetration level and installation patterns of RES.

Index Terms—DigSILENT PowerFactory, IEEE-33 bus, Power Quality, Renewable Energy Sources.

1 INTRODUCTION

RES form a critical part of African economies energy mix. Tremendous growth of RES in energy generation is expected as more African countries seek alternatives to fossil fuels which form part of their primary sources of energy. Usage of RES will not only make African economies less vulnerable to constantly changing prices of imported fossil fuels, but will also create new job opportunities, generate electricity close to load center and also address greenhouse gas emission concerns [1]. Further benefits of using RES for energy generation can be found in [2] and [3]. RES abundantly found in Africa include solar, wind, biogas, hydro, biomass and geothermal [4]. Greater attention is being given to wind and solar since they are technically feasible [5]. In addition, harnessing energy from the two sources is environmentally friendly and is not affected by changing climatic conditions.

RES are integrated into power networks at distribution network level. Gharehpetian and Mousavi [6] denote that this integration takes place at 400V for low voltage (LV) networks and between 11kV and 33kV for medium voltage(MV) networks. Energy generated from the RES is within kW-MW range and researchers consider different production amounts [6], [7]. Integration of RES on power system networks however causes issues in planning and operation of distribution grids [8], [9]. Operation concerns influenced by integration of RES include voltage control, fault level, power quality, grid losses and protection [10]. The impact on the operation of distribution networks depends on the type of RES and also whether the RES was integrated at MV or LV.

This paper assesses the effects of integrating wind and solar energy systems on operation of distribution networks with a special focus on harmonics and flicker which are key aspects of power quality. Wind and solar PV energy systems use power electronic devices (rectifiers and inverters) to interface the RES to the distribution grid that introduce significant levels of harmonic distortion. The operation of wind and solar PV energy systems also contribute dynamic voltage variations due to their frequent start and stop, and unceasing variation in input power caused by fluctuating energy source that result in voltage flicker [11].

To assess the impact of harmonic and flicker caused by the integration of wind and solar energy systems in the IEEE-33 bus, DigSILENT PowerFactory software was used due to its abilities of measuring harmonic distortion (HD and THD) and flicker indices (short and long-term flicker perceptions) at points of common coupling (PCC) through harmonic load flow and flicker analysis tools. Locations of the IEEE-33 bus selected for RES connection were buses 6 for single connection and buses 6 and 15 for two separate connections. This is in line with studies conducted by Prassana et al and Kumar et al [12], [13] who in their findings identified this two buses to be the optimal locations for integrating RES in order to reduce active power losses. Three connection scenarios were considered for this study. For the first case, each RES was connected to each bus at a time. In the second scenario, two separate generators of each source were connected to buses 6 and 15. For the third scenario, the RES were connected interchangeably to buses 6 and 15. In this study, LV buses voltage level was considered to be 1kV and below and for MV above 1kV. The rest of this paper is organized as follows: Section 2 gives the related works carried out on this subject, section 3 gives the models of solar and wind energy systems developed for this study, section 4 gives the simulation results and discussion and section 5 gives the conclusion.

2 RELATED WORKS

Authors in [14], [15], [16], [17] have analyzed the harmonic impact of integration of RES into distribution networks. From their findings, the levels of harmonic content is directly proportional to the scale of integration. In addition, the level

- *Francis Itote is currently pursuing masters degree program in electrical engineering in Pan African University Institute of Basic Sciences, Technology and Innovation (PAUSTI), Kenya.*
- *E-mail: itotefrancis@gmail.com*

of harmonic distortion is also dependent on the location and type of RES integrated into the networks [18]. These factors need to be considered in the planning of distribution networks integrated with RES[19].

Authors in [19], [20], [21] explain that inverters used to integrate RES into distribution networks inject harmonic currents and voltages. Harmonics are also introduced by nonlinear loads using power electronic devices for switching[21], [22]. Harmonics lower the power quality of distribution networks and increase values of line currents which negatively affects performance of end user equipment.

Voltage fluctuations that cause flicker result when RES of large capacity are integrated to weak grids [23], [24]. Factors that influence flicker emission in wind turbines include control strategies of the wind generator, windspeed , turbulence intensity and short circuit ratio at PCC [25], [26], [27]. Windfarms using the DFIG wind turbine technology were also found to produce less flicker compared to those using permanent magnet synchronous generator due to their two paths of controlling active and reactive power [28]. For solar PV, flicker is influenced by the inverter control characteristics, temperature and irradiance. A study by[29] denotes that solar PV systems emit less flicker and the levels do not exceed prescribed limits.

3 MODELLING OF RES

3.1 Modelling of solar PV system

Solar cells convert energy from sunlight to electrical energy using photovoltaic effect. Several models exist for modelling the solar cell across literature, however, the single diode model(SDM) is the most preferred due to its simplicity[30], [31]. The SDM solar cell consists of series and shunt resistors, current source and a diode. The terminal current of the SDM solar cell described by Fig 1 can be determined by subtracting the current passing through the diode and resistances [30], [32].

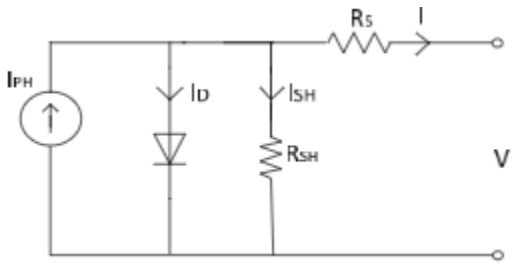

Fig 1. SDM solar cell equivalent circuit.

$$i = I_{ph} - I_D - I_{sh} \quad (1)$$

where i represents the load current, I_{ph} is the photocurrent, I_D is the diode current and I_{sh} is the current flowing in the shunt resistance. Elaboration of Equation (1) yields Equation (2).

$$i = I_{ph} - I_O.\left(e^{\frac{q(V+i.R_S)}{AKT}} - 1\right) - (V + IR_s)/R_p \quad (2)$$

where I_O represent the reverse saturation current of diode, $R_s$is the series resistance, R_p is the shunt resistance, V is the terminal voltage, q is the electron charge, K is the Boltzmann's constant and T is the absolute temperature of the solar cell.

In practical applications, the PV arrays constitute of PV cells connected in parallel or series to meet requirements of the SPV system [33], [34]. Series connection increases the output voltage and on the other hand, the parallel connection increases the output current. SPV are designed to operate either as stand-alone or grid-tied. Stand-alone SPV systems operate independent of the grid while on the other hand grid-tied SPV system operate parallel with the grid. For this study the grid-tied SPV system design without a battery back-up is considered. Authors in [35], [36] explains the layout of a grid-tied SPV system and various ways in which the inverter can be interconnected. The inverter can be centrally connected whereby one inverter is used to connect the entire PV system. Each PV module string can also be connected to its own inverter forming string inverters and another connection involves using micro-inverters whereby each PV module is connected to its own inverter.

To develop the SPV system in DigSILENT PowerFactory the static generator model is used as it has non-rotating parts. The solar PV system developed is illustrated by Fig 2 and generated 0.5Mw at 50Hz and at a voltage level of 0.4kV. In order to carry out harmonic simulations in DigSILENT PowerFactory, SPV systems are usually modelled to inject harmonic current spectrums. The developed SPV system inverter was assumed to inject the current harmonic spectrum in Table 1. The harmonic spectrum data is based on published results of a real PV installation whose capacity is 0.95MVA [37]. The flicker coefficients assigned to the developed SPV system are shown in Table 2.

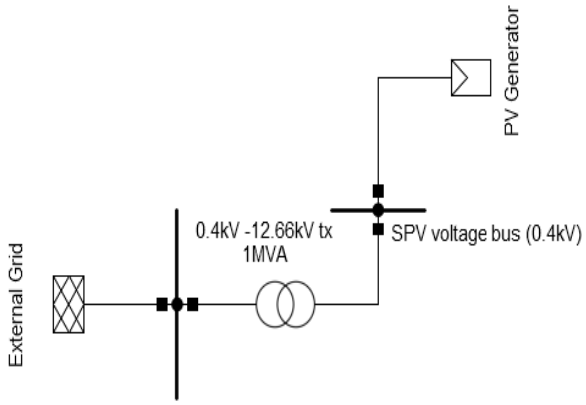

Fig 2. Developed solar PV system.

TABLE 1. HARMONIC CURRENT SPECTRUM OF SPV SYSTEM

Harmonic order (f/fn)	Magnitude %
3	1.28
5	3.78
7	1.53
9	0.38
11	0.37
13	0.37

TABLE 2. SOLAR PV SYSTEM FLICKER COEFFICIENTS

	Network angle, psi deg	Coefficient, c(psi)	Stepfactor, kf(psi)	Voltage change factor, ku(psi)
1	30	0.4	0.11	0.12
2	50	0.32	0.1	0.09
3	70	0.23	0.07	0.08
4	90	0.43	0.06	0.05

3.2 Modelling of DFIG wind turbine generator (DFIG WTG)

Wind energy conversion systems convert kinetic energy of moving air mass into mechanical energy. Generators are used to convert the mechanical power harnessed from wind into electrical power [38]. The instantaneous power of an air mass flowing through an area A at a speed V can be expressed as

$$P_{wind} = \frac{1}{2}\rho A V^3 \quad (3)$$

where ρ represents air density, A is the area swept across by wind and V is the speed of wind.

The theoretical maximum amount of wind power extracted by wind turbine according to Betz is a function of the power coefficient (C_p) of the rotor.

$$P_{betz} = \frac{1}{2}\rho A V^3 C_p \quad (4)$$

where P_{betz} represents maximum of the wind turbine, C_p is the rotor power coefficient (C_p = 0.59).

The wind turbine model considered for this study utilizes the doubly-fed inductor generator (DFIG). DFIG based wind turbines are the most dominant in wind generation systems. This is due to their numerous advantages including its ability to control reactive power and separate control of active and reactive power by autonomous control of rotor excitation current. Furthermore, DFIG can be magnetized from its rotor circuitry [38]. In DFIG systems, the stator voltage applied from the grid as it is directly connected whereas the voltage in the rotor is fed from the power electronic converter. The layout of the DFIG system is given in [39]. The back to back (AC-DC-AC) converter allows for bidirectional power flow as well as controlling the speeds of the DFIG system in super and sub-synchronous speed ranges. Using the dq reference frame, stator and rotor voltage equations used to model the DFIG are given by [40], [41]

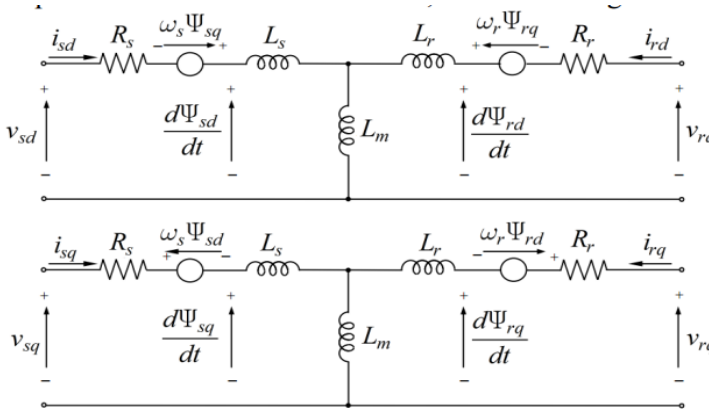

Fig 1. DFIG model equivalent circuit in dq reference frame [40].

$$V_{sd} = R_s I_{sd} + \frac{d\psi_{sd}}{dt} - \omega_s \psi_{sq} \quad (5)$$

$$V_{sq} = R_s I_{sq} + \frac{d\psi_{sq}}{dt} + \omega_s \psi_{sd} \quad (6)$$

$$V_{rd} = R_r I_{rd} + \frac{d\psi_{rd}}{dt} - \omega_r \psi_{rq} \quad (7)$$

$$V_{rq} = R_r I_{rq} + \frac{d\psi_{rq}}{dt} + \omega_r \psi_{rd} \quad (8)$$

Flux equations in the dq reference frame are

$$\psi_{sd} = (L_m + L_s) i_{sd} + M i_{rd} \quad (9)$$

$$\psi_{sq} = (L_m + L_s) i_{sq} + M i_{rq} \quad (10)$$

$$\psi_{rd} = (L_m + L_r) i_{rd} + M i_{sd} \quad (11)$$

$$\psi_{rq} = (L_m + L_r) i_{rq} + M i_{sq} \quad (12)$$

where M represents the mutual inductance L_m

The expression for electromagnetic torque for this model is described by

$$T_e = \frac{3}{2}\rho \frac{M}{(L_m + L_s)} (\psi_{sq} i_{rd} - \psi_{sd} i_{rq}) \quad (13)$$

The wind turbine generator system shown in Fig 4. was built using the 0.69kV, 1.0MW DFIG WTG template available in DigSILENT PowerFactory library. The developed DFIG WTG system was configured to generate 0.5MW at 50Hz and unity power factor. The DFIG WTG was assumed to inject the current harmonic spectrum of a Vestas V90/2000kW wind turbine converter described by Table 3 [42]. The DFIG WTG was also assigned flicker coefficients in Table 4 in order for it to contribute flicker in the power system.

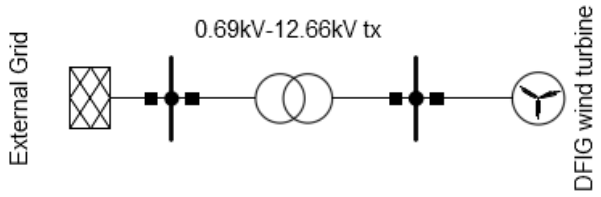

Fig 4. Developed DFIG WTG system.

TABLE 3. HARMONIC CURRENT SPECTRUM OF DFIG-WTG SYSTEM

Harmonic order (f/fn)	Magnitude %
1.5	0.513
2	0.715
5	0.446
5.5	0.927
7.5	0.665

TABLE 4. DFIG WIND TURBINE SYSTEM FLICKER COEFFICIENTS

	Network angle, psi deg	Coefficient, c(psi)	Stepfactor, kf(psi)	Voltage change factor, ku(psi)
1	30	2.7	0.09	0.91
2	50	4.5	0.12	0.72
3	70	6.4	0.14	0.35
4	85	7.5	0.17	0.24

4. RESULTS AND DISCUSSION

In this study, three different connections scenarios were analyzed to determine the contribution of wind and solar

energy sources to the harmonic content and flicker levels of the IEEE-33 bus. The bus and load data of the IEEE-33 bus distribution system can be found in [12]

4.1 Integration of wind and solar PV to bus 6 and 15 each bus at a time

In this connection scenario each RES source was individually connected to bus 6 and then to bus 15 to determine the level of harmonic and flicker each source introduced in the distribution system. Figs 5-8 shows the harmonic distortion plots of integrating SPV and DFIG-WTG systems individually to buses 6 and 15. From the simulated results, the THD values obtained at the PCC after integrating SPV system to buses 6 and 15 were 0.5% and 1.2% respectively. For the integration of the DFIG-WTG THD values obtained at PCC were 0.2% for bus 6 and 0.4% for bus 15. From the distortion plots as well as the values of the THD at PCC, the harmonic distortion introduced due to the integration of SPV and DFIG-WTG systems was within the prescribed IEEE 519-2014 limits for MV networks. Table 5 shows the measured short (Pst) and long-term (Plt) flicker perceptions for switching and continuous operations after the integration of SPV and DFIG-WTG systems. From the simulated results, the short and long-term flicker introduced by the integration of SPV and DFIG-WTG systems was within the compatibility levels for MV networks as prescribed by the IEC 61000-3-7 specification. From the simulation results, it is also evident that connecting either SPV or DFIG-WTG at bus 15 introduces higher levels of harmonic distortion and flicker emission.

TABLE 5 SHORT AND LONG-TERM FLICKER FOR SWITCHING AND CONTINUOUS OPERATION FOR SCENARIO 1.

RES type	Bus no	Pst (sw)	Plt (sw)	Pst (cont)	Plt (cont)
SPV	Bus 6	0.0751	0.0558	0.0085	0.0085
	Bus 15	0.2356	0.1750	0.0290	0.0290
DFIG-WTG	Bus 6	0.0939	0.0565	0.1447	0.1447
	Bus 15	0.2314	0.1394	0.3123	0.3123

4.2 Integration of two separate wind or solar PV generators of the same capacity to buses 6 and 15

In this scenario, two types of connections were made. In first connection two 0.5MW SPV generators were connected to buses 6 and 15 at the same time. For the second connection, the two SPV generators were replaced by DFIG-WTG of the same capacity. Figs 9-10 shows the harmonic distortion plots at the PCC for the two connections. The values of THD obtained after integrating SPV system to buses 6 and 15 are 0.9% and 1.5% respectively. For the DFIG-WTG integration THD values obtained were 0.3% and 0.5% for bus 6 and 15 respectively. These values were higher than when either source was integrated at each bus a time. The increase in harmonic distortion is also evident by the increased magnitudes of individual harmonics in Figs 9-10 when compared to Figs 5-8 for each of the two RES types. The level of harmonic distortion introduced by the two types of connection at the PCC was within the 5% limit set by IEEE 519-2014 standard for MV networks. Table 6 shows the measured short (Pst) and long-term (Plt) flicker perceptions for switching and continuous operations for the two connections. From the results of Tables 5 and 6, the level of flicker emitted after the integration of either type of RES increased as more generators of the same RES type were connected to the IEEE-33 bus system. The DFIG-WTG system was also found to emit higher levels of flicker than the SPV system during continuous operation. The values of short and long-term flicker perceptions obtained for the two connection types were within the compatibility levels set by IEC 61000-3-7 standards.

TABLE 6 SHORT AND LONG-TERM FLICKER PERCEPTIONS FOR SWITCHING AND CONTINUOUS OPERATION FOR SCENARIO 2.

RES connection	Bus no	Pst (sw)	Plt (sw)	Pst (cont)	Plt (cont)
SPV to buses 6 and 15	6	0.0917	0.0682	0.0119	0.0119
	15	0.2374	0.1764	0.0302	0.0302
DFIG-WTG to buses 6 and 15	6	0.1143	0.0689	0.2010	0.2010
	15	0.2350	0.1416	0.3423	0.3423

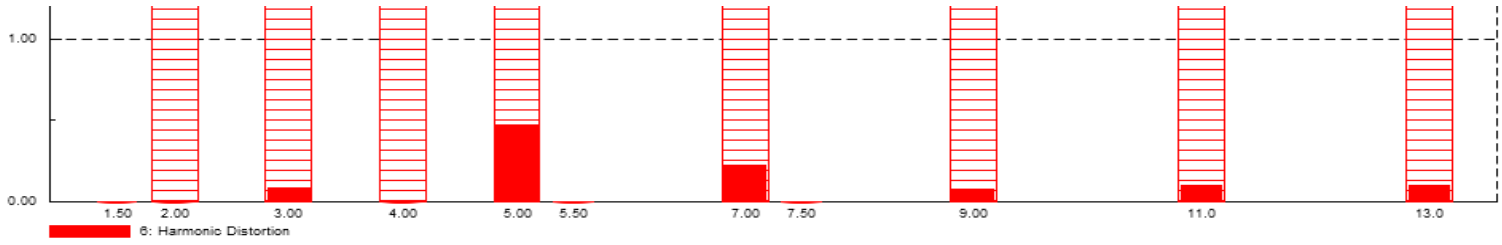

Fig 5..: HD of integrating SPV system at bus 6.

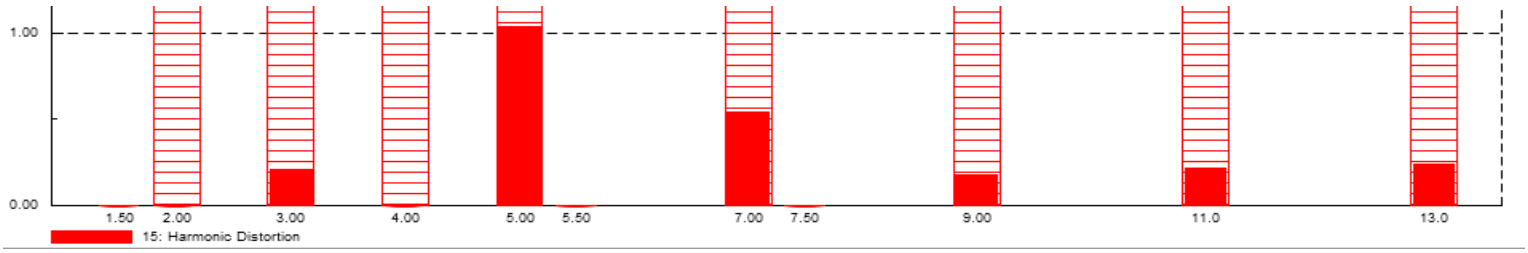

Fig *6.* HD of integrating SPV system at bus 15.

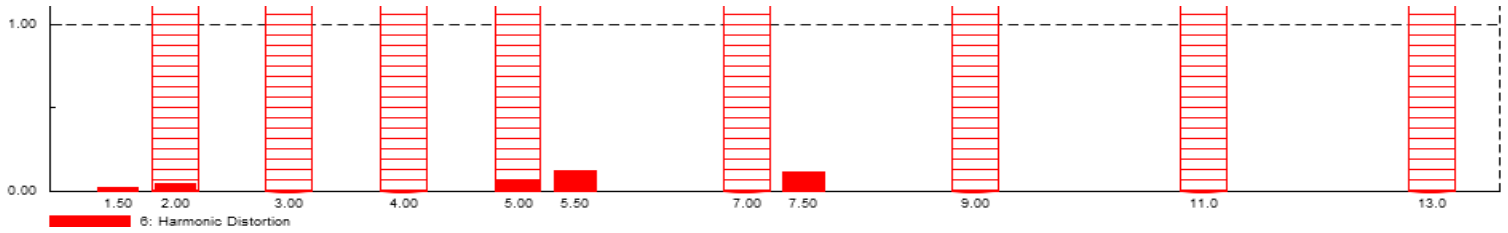

Fig 2: HD of integrating DFIG-WTG system at bus 6.

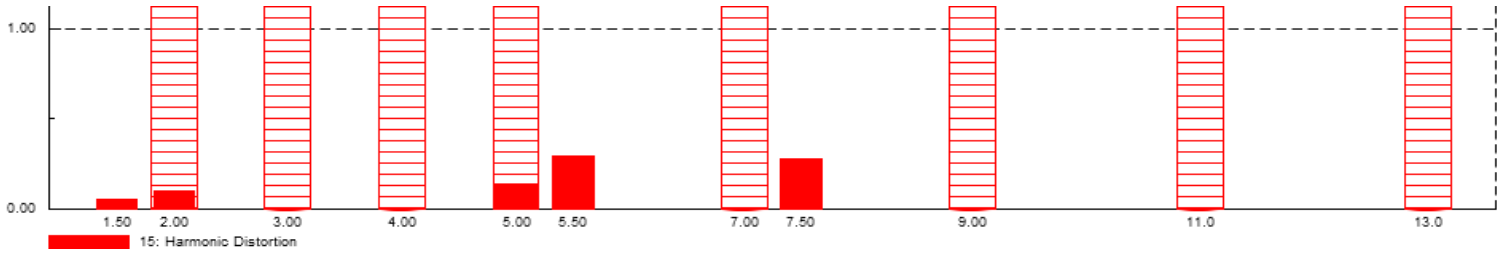

Fig 3.: HD of integrating DFIG-WTG system at bus 15.

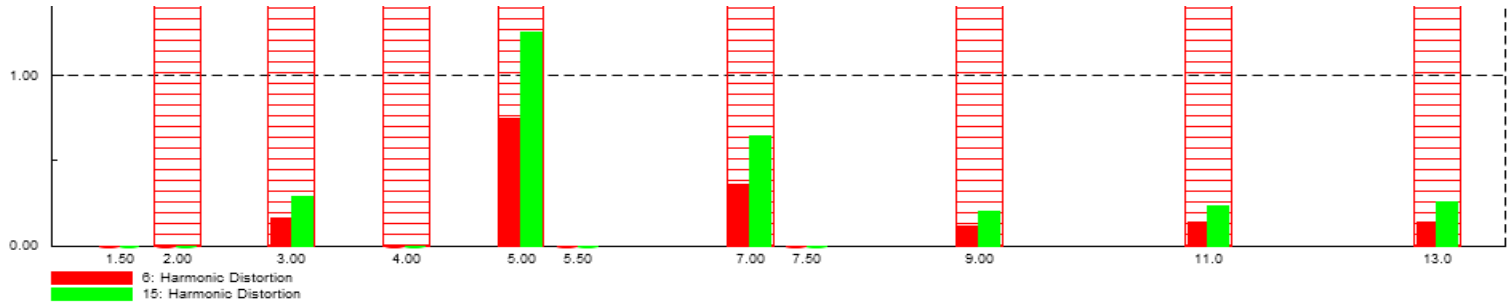

Fig 4.: HD of integrating SPV system at bus 6 and 15

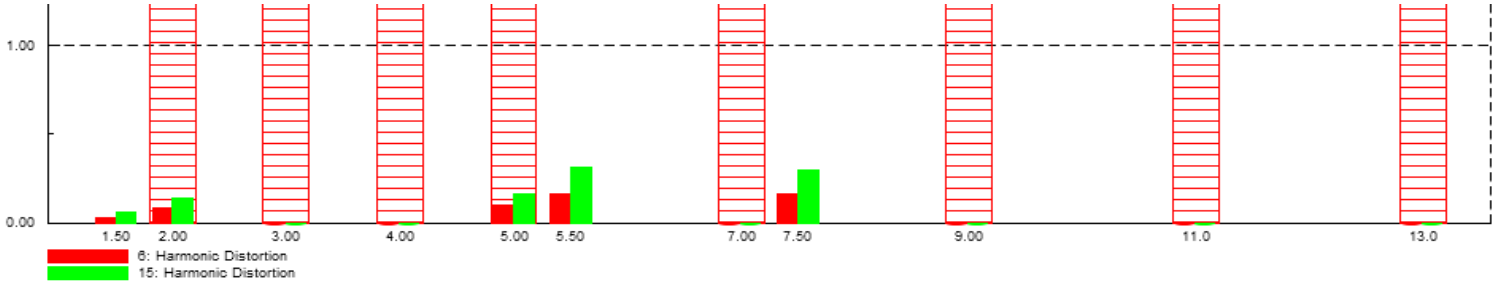

Fig 5.: HD of integrating DFIG-WTG system at bus 6 and 15.

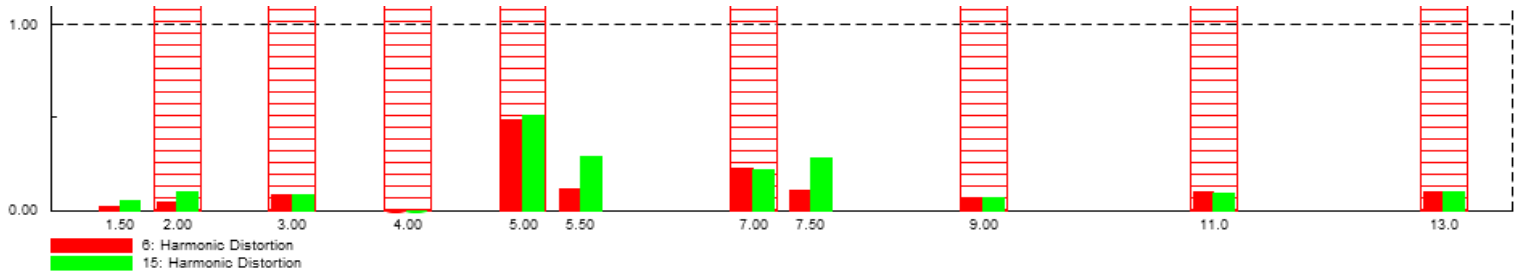

Fig 6.: HD of integrating SPV to bus 6 and DFIG-WTG to bus 15 .

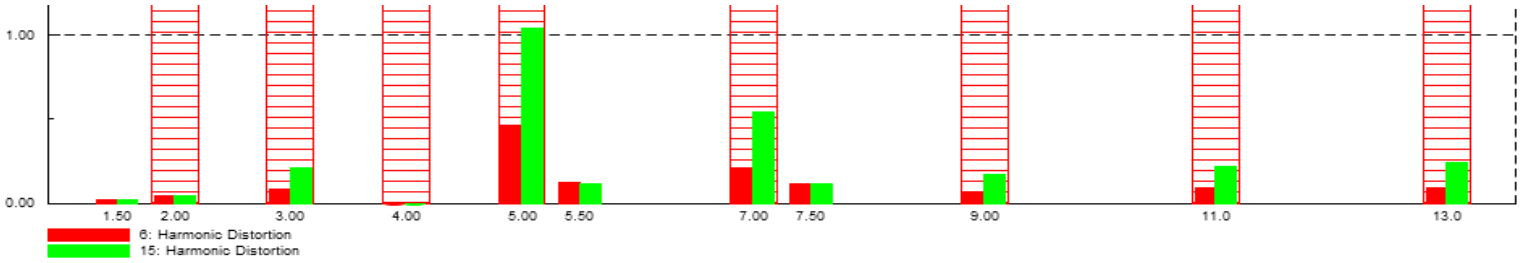

Fig 7.: HD of integrating DFIG-WTG to bus 6 and SPV to bus 15

4.3 Integration of wind and solar PV generators at buses 6 and 15 interchangeably

In this scenario two separate connections were considered. In the first connection the SPV system was placed at bus 6 and DFIG-WTG at bus 15 of the IEEE-33 bus system. For the second connection the two RES types were swapped and the DFIG-WTG was placed at bus 6 and SPV system at bus 15. Figs 11-12 illustrate the harmonic distortion plots at the PCC for the two connections. The measured value of THD at PCC for the first connection were 0.6% for bus 6 and 0.7% for bus 15. For the second connection the obtained THD values were 0.6% for bus 6 and 1.3% for bus 15. It is evident that the values of THD obtained decreased when a combination of the DFIG-WTG and SPV systems was connected to buses 6 and 15 compared to the integration of two separate SPV generators at buses 6 and 15 of the IEEE-33 bus. The best combination scenario was the first connection due to the low values of THD and HD as illustrated by Fig 11. In the two connections considered for scenario 3, the values of THD obtained were within the 5% limit set by IEEE 519-2014 standards. Table 7 shows the measured short (Pst) and long-term (Plt) flicker perceptions for switching and continuous operations for the two connections under consideration. These values were within the compatibility levels set by IEC 61000-3-7 standards for MV networks.

TABLE 7. : SHORT AND LONG-TERM FLICKER FOR SWITCHING AND CONTINUOUS OPERATION FOR SCENARIO 3.

RES connection	Bus no	Pst (sw)	Plt (sw)	Pst (cont)	Plt (cont)
SPV to bus 6 and DFIG-WTG to bus 15	6	0.1035	0.0684	0.1393	0.1393
	15	0.2334	0.1415	0.3128	0.3128
DFIG-WTG to bus 6 and SPV to bus 15	6	0.1052	0.0687	0.1452	0.1452
	15	0.2391	0.1765	0.1413	0.1413

5. CONCLUSION

The impact on harmonics and flicker of the IEEE 33 bus after integration of RES has been studied and THD and short and long-term flicker perceptions measured at medium voltage. The results indicate that the level of harmonic distortion and flicker emitted increases with the penetration level of the SPV and DFIG-WTG systems into the distribution network. Amount of THD and flicker introduced into the distribution network also depends on the type of RES. From the simulations it was established that the level of harmonic distortion and flicker was within the limits prescribed by the IEEE 519-2014 and IEC 61000-3-7 standards. Furthermore, it was established that the integration of the same type of RES produced higher THD than a combination of various RES types.

ACKNOWLEDGMENTS

This research work forms part of postgraduate research work and is supported by the Pan African University Institute of Basic Sciences, Technology and Innovation (PAUSTI).

REFERENCES

[1] A. K. Aliyu, B. Modu, and C. W. Tan, "A review of renewable energy development in Africa: A focus in South Africa, Egypt and Nigeria," Renew. Sustain. Energy Rev., vol. 81, pp. 2502–2518, Jan. 2018.

[2] A. González, J.-R. Riba, A. Rius, and R. Puig, "Optimal sizing of a hybrid grid-connected photovoltaic and wind power system," Appl. Energy, vol. 154, pp. 752–762, Sep. 2015.

[3] J. Mohtasham, "Review Article-Renewable Energies," Energy Procedia, vol. 74, pp. 1289–1297, Aug. 2015.

[4] B. Kichonge, I. S. N. Mkilaha, G. R. John, and S. Hameer, "The Economics of Renewable Energy Sources into Electricity Generation in Tanzania," J. Energy, vol. 2016, pp. 1–8, Jul. 2016.

[5] M. S. Okundamiya, J. O. Emagbetere, and E. A. Ogujor, "Assessment of renewable energy technology and a case of sustainable energy in mobile telecommunication sector.," ScientificWorldJournal., vol. 2014, p. 947281, Jan. 2014.

[6] G. B. Gharehpetian and S. M. Mousavi Agah, Distributed generation systems : design, operation and grid integration, 1st ed. Kidlington, Oxford, United Kingdom: Butterworth-Heinemann(imprint of Elsevier), 2017.

[7] V. S. Bhadoria, N. S. Pal, and V. Shrivastava, "A Review on Distributed Generation Definitions and DG Impacts on Distribution System," in International Conference on Advanced Computing and Communication Technologies (ICACCT), 2013.

[8] E. J. Coster, J. M. A. Myrzik, B. Kruimer, and W. L. Kling, "Integration Issues of Distributed Generation in Distribution Grids," Proc. IEEE, vol. 99, no. 1, pp. 28–39, Jan. 2011.

[9] E. De Jong and P. Vaessen, "The impact of large-scale PV on distribution grid operation and protection; and appropriate testing," in CIRED 2012 Workshop: Integration of Renewables into the Distribution Grid, 2012, pp. 82–82.

[10] T. Ackermann and V. Knyazkin, "Interaction between distributed generation and the distribution network: operation aspects," in IEEE/PES Transmission and Distribution Conference and Exhibition, 2002, vol. 2, pp. 1357–1362.

[11] A. Hamzeh and A. Sandouk, "Impact of Integrated Hybrid PV/Wind Generation on Harmonic Power Flow in Medium-Voltage Grid," in Renewable Energy in the Service of Mankind Vol II : Selected Topics from the World Renewable Energy Congress WREC 2014, 1st ed., A. Sayigh, Ed. Cham: Springer International Publishing, 2016, pp. 81–92.

[12] K. M. L. Prasanna, A. Jain, and R. J. R. Kumar, "Optimal Distributed Generation Placement Using Hybrid Technique," in 2017 IEEE PES Asia-Pacific Power and Energy Engineering Conference (APPEEC), 2017, pp. 1–6.

[13] A. Kumar and R. T. Bhimarasetti, "Multiple Distribution Generation Location in Reconfigured Radial Distribution System Distributed generation in Distribution System," in 2nd International Conference on Energy and Environmental Science, 2018, vol. 164, p. 012011.

[14] G. M. Shafiullah and A. M. T. Oo, "Analysis of harmonics with renewable energy integration into the distribution network," in 2015 IEEE Innovative Smart Grid Technologies - Asia (ISGT ASIA), 2015, pp. 1–6.

[15] N. Mithulananthan, T. Kumar Saha, and A. Chidurala, "Harmonic impact of high penetration photovoltaic system on unbalanced distribution networks – learning from an urban photovoltaic network," IET Renew. Power Gener., vol. 10, no. 4, pp. 485–494, 2016.

[16] M. Vukobratović, P. Marić, S. Nikolovski, and H. Glavaš, "Distributed Generation Harmonic Interaction in the Active Distribution Network," Teh. Vjesn. - Tech. Gaz., vol. 25, no. 6, pp. 1720–1730, Dec. 2018.

[17] J. A. Sa'ed, M. Quraan, Q. Samara, S. Favuzza, and G. Zizzo, "Impact of integrating photovoltaic based DG on distribution network harmonics," in 2017 IEEE International Conference on Environment and Electrical Engineering and 2017 IEEE Industrial and Commercial Power Systems Europe (EEEIC / I&CPS Europe), 2017, pp. 1–5.

[18] A. F. A. Kadir, A. Mohamed, and H.Shareef, "Harmonic impact of different distributed generation units on low voltage distribution system," in 2011 IEEE International Electric Machines & Drives Conference (IEMDC), 2011, pp. 1201–1206.

[19] A. F. Abdul Kadir, T. Khatib, and W. Elmenreich, "Integrating Photovoltaic Systems in Power System: Power Quality Impacts and Optimal Planning Challenges," Int. J. Photoenergy, vol. 2014, pp. 1–7, Aug. 2014.

[20] M. Karimi, H. Mokhlis, K. Naidu, S. Uddin, and A. H. A. Bakar, "Photovoltaic penetration issues and impacts in distribution network – A review," Renew. Sustain. Energy Rev., vol. 53, pp. 594–605, Jan. 2016.

[21] I. Bouloumpasis et al., "Current Harmonics Compensation in Microgrids Exploiting the Power Electronics Interfaces of Renewable Energy Sources," Energies, vol. 8, no. 4, pp. 2295–2311, Mar. 2015.

[22] Priyashree S, Pooja A B, Mahesh E, and Vidya H A, "Harmonic suppression in a non-linear load using three phase shunt active power filter," in 2016 Biennial International Conference on Power and Energy Systems: Towards Sustainable Energy (PESTSE), 2016, pp. 1–6.

[23] M. Bollen and F. Hassan, Integration of Distributed Generation in the Power System, 1st ed. Hoboken, NJ, USA: John Wiley & Sons, Inc., 2011.

[24] B. Fox et al., Wind Power Integration: Connection and System Operational Aspects, 2nd ed. London.UK: Institution of Engineering and Technology, 2014.

[25] L. Meegahapola and S. Perera, "Impact of wind generator control strategies on flicker emission in distribution networks," in 2012 IEEE 15th International Conference on Harmonics and Quality of Power, 2012, pp. 612–617.

[26] C. Vilar, J. Usaola, and H. Amaris, "A frequency domain approach to wind turbines for flicker analysis," IEEE Trans. Energy Convers., vol. 18, no. 2, pp. 335–341, Jun. 2003.

[27] T. Sun, Z. Chen, and F. Blaabjerg, "Flicker Study on Variable Speed Wind Turbines With Doubly Fed Induction Generators," IEEE Trans. Energy Convers., vol. 20, no. 4, pp. 896–905, Dec. 2005.

[28] I. A. Ahmed and A. F. Zobaa, "Comparative Power Quality Study of Variable Speed Wind Turbines," Int. J. Energy Convers., vol. 4, no. 4, pp. 97–104, Jul. 2016.

[29] S. B. Kjær, "Flicker and Photovoltaic Power Plants," in 25th European Photovoltaic Solar Energy Conference and Exhibition / 5th World Conference on Photovoltaic Energy Conversion, 2010, pp. 4997–4999.

[30] Y. Yoon and Z. W. Geem, "Parameter Optimization of

Single-Diode Model of Photovoltaic Cell Using Memetic Algorithm," Int. J. Photoenergy, vol. 2015, pp. 1–7, Nov. 2015.

[31] W. Xiao, Photovoltaic Power System, 1st ed. Hoboken, NJ, USA: John Wiley & Sons, Inc., 2017.

[32] J. Ma, K. L. Man, T. O. Ting, N. Zhang, S.-U. Guan, and P. W. H. Wong, "Approximate single-diode photovoltaic model for efficient I-V characteristics estimation.," ScientificWorldJournal., vol. 2013, p. 230471, Nov. 2013.

[33] H. Tian, F. Mancilla-David, K. Ellis, E. Muljadi, and P. Jenkins, "A cell-to-module-to-array detailed model for photovoltaic panels," Sol. Energy, vol. 86, no. 9, pp. 2695–2706, Sep. 2012.

[34] M. Sabbaghpur Arani and M. A. Hejazi, "The Comprehensive Study of Electrical Faults in PV Arrays," J. Electr. Comput. Eng., vol. 2016, pp. 1–10, Dec. 2016.

[35] N. Vázquez and J. Vázquez, "Photovoltaic System Conversion," in Power Electronics Handbook, 4th ed., M. H. Rashid, Ed. Butterworth-Heinemann, 2018, pp. 767–781.

[36] L. El Chaar, "Photovoltaic System Conversion," in Alternative Energy in Power Electronics, 1st ed., M. H. Rashid, Ed. Butterworth-Heinemann, 2015, pp. 155–175.

[37] A. Varatharajan, S. Schoettke, J. Meyer, and A. Abart, "Harmonic Emission of Large PV Installations Case Study of a 1 MW Solar Campus," in International Conference on Renewable Energies and Power Quality (ICREPQ'14), 2014, vol. 1, no. 12, pp. 701–706.

[38] T. Ackermann, Wind Power in Power Systems, 2nd ed. Chichester, UK: John Wiley & Sons, Ltd, 2012.

[39] M. Ahmad, Operation and Control of Renewable Energy Systems, 1st ed. Chichester, UK: John Wiley & Sons, Ltd, 2017.

[40] M. Sleiman, B. Kedjar, A. Hamadi, K. Al-Haddad, and H. Y. Kanaan, "Modeling, control and simulation of DFIG for maximum power point tracking," in 2013 9th Asian Control Conference (ASCC), 2013, pp. 1–6.

[41] O. Zamzoum, Y. El Mourabit, A. Derouich, and A. El Ghzizal, "Study and implementation of the MPPT strategy applied to a variable speed wind system based on DFIG with PWM-vector control," in 2016 International Conference on Electrical Sciences and Technologies in Maghreb (CISTEM), 2016, pp. 1–6.

[42] K. Yang, "Wind Turbine Harmonic Emissions and Propagation through A Wind Farm," Lule˚a University of Technology Sweden, 2012.